Helicobacter pylori Cytotoxin-Associated Gene A Activates the Signal Transducer and Activator of Transcription 3 Pathway *In vitro* and *In vivo*

Dana M. Bronte-Tinkew,[1,2,3] Mauricio Terebiznik,[1,2,3] Aime Franco,[4] Michelle Ang,[1,2,3] Diane Ahn,[1,2,3] Hitomi Mimuro,[5] Chihiro Sasakawa,[5] Mark J. Ropeleski,[6] Richard M. Peek, Jr.,[4] and Nicola L. Jones[1,2,3]

[1]Department of Pediatrics and Physiology, University of Toronto; [2]Cell Biology Program, Research Institute and [3]Division of Gastroenterology, Hepatology and Nutrition, Hospital for Sick Children, Toronto, Canada; [4]Division of Gastroenterology, Departments of Medicine and Cancer Biology, Vanderbilt University School of Medicine, Nashville, Tennessee; [5]Department of Microbiology and Immunology, Institute of Medical Science, University of Tokyo, Tokyo, Japan; and [6]Division of Gastroenterology, Departments of Medicine and Anatomy and Cell Biology, Queen's University, Kingston, Canada

Abstract

Persistent infection with *Helicobacter pylori* confers an increased risk for the development of gastric cancer. However, the exact mechanisms whereby this bacterium causes carcinogenesis have not been completely elucidated. Recent evidence indicates that aberrant activation of the signal transducers and activators of transcription 3 (STAT3) signaling pathway may play a role in gastric carcinogenesis. Therefore, we hypothesized that *H. pylori* infection modulates STAT3 signaling, favoring gastric cancer development. In epithelial cells infected with *H. pylori*, STAT3 was activated, as assessed by immunoblotting for phosphorylated STAT3, immunofluorescence of translocated STAT3, fluorescence recovery after photobleaching, and luciferase activation in transfected cells. Activation was dependent on translocation but not phosphorylation of cytotoxin-associated gene A (CagA) in host cells. Activation seemed to be receptor-mediated because preincubation of cells with the interleukin-6 (IL-6) receptor superantagonist sant7 or inhibition of gp130 by a monoclonal antibody prevented *H. pylori*–mediated STAT3 activation. However, activation was not related to autocrine activation by IL-6 or IL-11. CagA+ wild-type *H. pylori*, but not the noncarcinogenic *cagA*− mutant, activated STAT3 in gastric epithelial cells *in vivo* in the gerbil model of *H. pylori*–mediated gastric carcinogenesis. Collectively, these results indicate that *H. pylori* CagA activates the STAT3 signaling pathway *in vitro* and *in vivo*, providing a potential mechanism by which chronic *H. pylori* infection promotes the development of gastric cancer. [Cancer Res 2009;69(2):632–9]

Introduction

Gastric cancer is the second most common cause of cancer-related deaths worldwide, accounting for greater than 1 million deaths per year (1). Infection with *Helicobacter pylori* is the major predisposing factor for the development of gastric adenocarcinomas (1, 2). Individuals infected with strains containing the cytotoxin-associated gene A (CagA) have an increased risk for developing gastric cancer compared with those infected with *H. pylori* strains lacking the CagA protein (1, 2). Upon infection, CagA is injected into host epithelial cells via a type IV secretion system (1, 3). Injected CagA localizes to the host cell membrane, where it is targeted for tyrosine phosphorylation within a repeated specific five–amino acid EPIYA motif (3). Once phosphorylated, CagA binds to a SRC homology 2 (SH2) domain-containing protein tyrosine phosphatase SHP2, activating its phosphatase activity and forming a complex that initiates mitogenic signaling and cell morphologic changes, involving rearrangement of the actin cytoskeleton (1). CagA is also able to bind, independent of its tyrosine phosphorylated EPIYA domain, to other host signaling molecules, including growth factor receptor binding protein 2 (Grb2) and c-MET receptors (4, 5). CagA, independent of tyrosine phosphorylation, interacts with ZO-1 and junctional adhesion molecule (JAM), forming a complex that alters tight junctions (6). CagA can, therefore, interact with intracellular signaling pathways in both a tyrosine phosphorylation–dependent and tyrosine phosphorylation–independent manner to perturb cellular homeostasis. Despite these elegant studies defining CagA-host cell interactions, the exact mechanism by which CagA promotes carcinogenesis is not known.

Current evidence indicates that signal transducers and activators of transcription 3 (STAT3) may be involved in the development of gastric cancer. STAT proteins are a family of latent transcriptional factors that exist as monomers within the cytoplasm of cells (7, 8). STAT3 can be activated by a number of different cytokines, including interleukin-6 (IL-6), IL-11, ciliary neurotrophic factor, oncostatin M, and leukemia inhibitory factor, which all signal through a shared gp130 signal transducer receptor subunit. IL-6–induced STAT3 activation involves binding of cytokine molecules to a membrane-bound glycoprotein IL-6 receptor (IL-6R) chain on target cells triggering heterodimerization with gp130, followed by activation of gp130 receptor-associated Janus-activated kinase (JAK) kinase. Latent STAT3 monomers are then recruited to the phosphorylated residues of the gp130 receptor, phosphorylated by JAK1 and JAK2 on single tyrosine resides (Tyr^{705}), resulting in their dimerization via reciprocal SH2 phosphorylated tyrosine interactions. Dimeric STAT3 then translocates to the nucleus, where it up-regulates the transcription of various genes involved in growth and proliferation.

Numerous studies indicate that STAT3 plays a key role in promoting oncogenesis. STAT3 is constitutively activated in a variety of human neoplasms (7, 8). The development of tumors in nude mice in gain-of-function studies confirms the role of STAT3 as an oncogene (9). STAT3 activation is implicated in all aspects of

Note: Supplementary data for this article are available at Cancer Research Online (http://cancerres.aacrjournals.org/).

Requests for reprints: Nicola L. Jones, Departments of Physiology and Pediatrics, Hospital for Sick Children, 555 University Avenue, Toronto, M5G 1X8, Canada. Phone: 416-813-7062; Fax: 416-813-6531; E-mail: nicola.jones@sickkids.ca.

doi:10.1158/0008-5472.CAN-08-1191

carcinogenesis, including cell proliferation, apoptosis, angiogenesis, invasion, migration, and disruption of immune surveillance (7, 8). With respect to gastric neoplasia, STAT3 is constitutively phosphorylated in various gastric cancer cell lines (10). In addition, *in vivo* evidence supports a role for STAT3 activation in gastric carcinogenesis. In this robust model, mice harboring a knock-in mutation in the gp130 receptor subunit that results in constitutive up-regulation of JAK-STAT3 spontaneously develop antral tumors by 4 weeks of age (11, 12). Furthermore, recent evidence indicates that a threshold level of STAT3 activation is required to promote tumor initiation in this model (13). Thus, there is an increasing body of evidence indicating that aberrant STAT3 activation is involved in the development of gastric cancer. Because the majority of gastric cancers occur as a result of *H. pylori* infection, we have explored the effect of *H. pylori* infection on STAT3 activation, both *in vitro* and *in vivo*. Furthermore, the role of the cancer-associated effector protein CagA and the potential molecular mechanisms involved were defined.

Materials and Methods

Cell cultures. HEp-2 cells (ATCC CCL 23, purchased from American Type Culture Collection), INT 407, and HeLa cells were cultured in Eagle's MEM with Earle's salts and L-glutamine (Wisent, Inc.) and supplemented with 10% heat-inactivated fetal bovine serum (Bethesda Research Laboratories-Life Technologies) and 1% penicillin streptomycin.

***H. pylori* strains and infection conditions.** *H. pylori* strain 60190 (ATCC 43526, *cagA+, cagE+, vacA+*) and its corresponding isogenic *cagA−*, *cagE−*, strain 251, and its TFSS mutant *cagM* (provided by Dr. A. Labigne, Pasteur Institute); strain G27 and the CagA EPISA mutant (provided by Dr. M. Amieva); and gerbil adapted strain 7.13 or the corresponding isogenic *cagA−* 7.13 mutant were used in these studies and cultured as described previously (for strains used, see Supplementary Table S1; refs. 6, 14). In some experiments, *H. pylori* was heat killed by boiling for 15 min in sealed, sterile Eppendorf tubes. Heat killing was confirmed by lack of growth on Columbia agar plates. HEp-2 cells or epithelial cells, as noted, were serum starved (24 h) and incubated with bacteria for up to 4 h at multiplicities of infection (MOI) of 50:1. Where indicated, 15 to 30 min before infection, cells were incubated with either an IL-6R antagonist, sant7 (ref. 15; 50 μg/mL, provided by Dr. M. Chatterjee, Humboldt University of Berlin), human anti-gp130 receptor antibody (50–100 μg/mL, Immunonokontact), or neutralizing anti–IL-6 antibody (50 ng/mL, Sigma Aldrich) for 15 min before infection.

Cell lysates and Western blotting. After 4 h of infection, cells were washed and scraped in 200 μL of radioimmunoprecipitation assay buffer (RIPA) buffer containing phosphatase and protease inhibitors (all obtained from Sigma Aldrich). Cell suspensions were centrifuged, and supernatants were stored at −70°C. Protein concentrations were measured using the Bio-Rad detergent-compatible protein assay. Whole-cell lysates (70 μg/mL) or nuclear extracts in Laemelli buffer were loaded onto 10% SDS-polyacrylamide separating gels and run at 110 V for 1.5 h at room temperature. Proteins were then transferred onto a nitrocellulose membrane (BioTrace NT, Pall Corp.). After blocking, membranes were incubated overnight with either rabbit anti–phosphorylated STAT3 (pSTAT3) antibody (1:250, Cell Signaling), rabbit anti–pSTAT3 (Ser^{727}) antibody (1:250, Cell Signaling), mouse anti-STAT3 antibody (1:500, Cell Signaling), mouse anti–phosphorylated tyrosine antibody (1:200, Upstate Cell Signaling Solutions), or mouse anti-CagA antibody (1:200, Santa Cruz Biotechnology) in TBST-milk. Blots were then incubated with the corresponding secondary horseradish peroxidase–conjugated antibody (The Jackson Laboratory; 1 h at room temperature). Bands were visualized by chemiluminesence using Kodak Biomax MR film.

Densitometric analysis. Densitometric analysis was performed using FluorChem FC11 software. All blots (*n* values) from each independent experiment were used. Densities of pSTAT3 and STAT3 bands were measured for each treatment and expressed as a ratio (pSTAT3/STAT3). For graphic representation, the ratio of pSTAT3 to STAT3 for each treatment was expressed relative to the measured ratio for control cells and identified as fold increase on graphs.

Coimmunoprecipitation. HEp-2 cells were grown to confluency on six-well plates and transfected with CagA-GFP or cotransfected with CagA-GFP and gp130-CFP. Whole-cell lysates were prepared, as previously described, and incubated overnight with either the anti-gp130, anti-CagA, or anti-GFP antibodies. Protein A Sepharose CL-4B beads were used to pull down the specific lysate-IgG antibody combinations. Immunoblotting was then performed with either anti-CagA (1:250, Santa Cruz Biotechnology), anti-gp130 (1:250, Upstate Cell Signaling Solutions), or anti-SHP-2 (1:500, Cell Signaling) antibodies.

Immunofluorescence and fluorescence microscopy. HEp-2 cells were seeded on glass coverslips and serum starved for 24 h. Cells were then incubated with either IL-6 (100 ng/mL) for 30 min or *H. pylori* for 4 h. After fixation, cells were permeabilized and blocked with 10% normal goat serum, and STAT3 was detected using a mouse anti-STAT3 antibody (1:100, Cell Signaling) and Cy3 donkey anti-mouse conjugated antibody (1:1,000, The Jackson Laboratory). Images were captured using an inverted Carl Zeiss META Laser Scanning Confocal Microscope. Analysis of relative fluorescence intensity was performed on cells using Image J software.

DNA transfections. Transient transfection of GFP, STAT3-GFP plasmids (a gift from Dr. K.Watanabe, Hokkaido University, Japan), and wild-type (wt) CagA-GFP constructs were performed in HEp-2 cells using the AMAXA Nucleofector System according to the procedure outlined (AMAXA Biosystems). Twenty hours posttransfection, whole-cell lysate extracts were collected.

ELISA. HEp-2 cells were grown to confluency in 6-well plates and infected with *H. pylori* wt strain 60190 for 4 h. Supernatants were collected and assayed for IL-6, IL-11, or human leukemia inhibitory factor (LIF) using specific ELISAs, as per the manufacturer's instructions (R&D Systems).

Fluorescence recovery after photobleaching. Fluorescence recovery after photobleaching was performed using an inverted confocal LSM 510 (Carl Zeiss) microscope equipped with an argon Laser. Coverslips with cells expressing STAT3-GFP constructs were mounted on the stage of the confocal microscope. After acquiring two baseline fluorescence measurements, the nucleus was bleached and the recovery in fluorescence of both areas is measured over time. The fractional fluorescence recovery was expressed relative to the initial fluorescence of the nucleus, and the changes in fluorescence that occurred in unbleached cytoplasm post bleaching. Mathematical treatment and modeling was performed using Graph Pad Prism (version 3.02).

Luciferase assays. The pSTAT3-luciferase reporter, which carries two tandem repeats of the acute phase response element of the α-2-macroglobulin and the p950M4/luciferase reporter, characterized by four copies of the STAT3-binding DNA element from the human angiotensinogen promoter (5′-CGTTTCTGGGAACCT-3′) cloned into pBL_2Luc (provided by Dr. Sehgal, New York Medical College) were transfected into HEp-2 cells using the Amaxa system (16). Transfected cells were incubated with IL-6 or infected with *H. pylori*, cell lysates collected and luciferase activity measured using a Promega dual luciferase kit. Assays were carried out at least in triplicate, and luciferase activity expressed in arbitrary units after normalization against *Renilla* luciferase activity.

***In vivo* infection of mongolian gerbils.** Male Mongolian gerbils (Harlan Labs) 4 to 8 wks of age were orogastrically challenged with either sterile *Brucella broth, H. pylori* strain 7.13, or an isogenic 7.13 *cagA* mutant, as described before (14). After 6 and 12 wk, animals were euthanized and the stomachs were collected and homogenized in RIPA buffer containing phosphatase and protease inhibitors. Gastric tissue lysates were probed via immunoblotting for changes in STAT3 activation using a rabbit anti-pSTAT3 antibody (1:250, Cell Signaling). All procedures were carried out with the approval of the Institutional Animal Care Committee of Vanderbilt University.

Immunohistochemistry. Four-micrometer-thick sections were cut from paraffin-embedded sections from control or *H. pylori*–infected gerbil stomachs. Paraffin-embedded tissue was rehydrated, and antigen unmasking was performed by boiling slides in 10 mmol/L Tris (pH 10.0). Sections

were fixed with 4% PFA and blocked in 5% donkey serum in 0.1% triton X. Overnight incubations in rabbit anti-pSTAT3 antibody (1:50, Cell Signaling), followed by 1 h secondary Cy3. A donkey anti-rabbit conjugated antibody incubations (1:500, The Jackson Laboratory) were performed. 4′,6-Diamidino-2-phenylindole (DAPI; 1:1,000) staining was done to identify nuclear compartments. Slides were mounted using DAKO. Consecutive tissue sections were stained with hemotoxylin and eosin and graded for chronic antral inflammation and colonization density, as described by Franco and colleagues (14).

Results

***H. pylori* triggers tyrosine phosphorylation of STAT3.** To determine if *H. pylori* induces tyrosine phosphorylation of STAT3 in epithelial cells, immunoblotting of cell lysates using a pSTAT3 antibody was performed. As described previously, AGS gastric epithelial cells display constitutively active STAT3 (10). Therefore, HEp-2 cells, which have been used previously as a model epithelium of signal transduction responses during *H. pylori* infection, which do not constitutively express activated STAT3, were used for the remainder of the studies. HEp-2 cells treated with IL-6 (positive control) displayed increased pSTAT3 in comparison with uninfected cells (Fig. 1). Similarly, HEp-2 cells infected with wt *H. pylori* strains 60190 (Fig. 1) and 7.13 (Supplementary Fig. S1) for 4 hours showed increased STAT3 phosphorylation in comparison with uninfected cells. In addition, the degree of phosphorylation of STAT3 increased with higher multiplicities of infection with strain 60190 (Supplementary Fig. S2). *H. pylori* also induced STAT3 phosphorylation in INT 407 cells (Supplementary Fig. S3) and HeLa cells (data not shown) indicating that this finding was not restricted to HEp-2 cells.

***H. pylori* infection induces nuclear translocation of STAT3.** Next, nuclear translocation of STAT3 was determined by STAT3 immunolabeling. Control cells displayed a greater distribution of STAT3 in the cytoplasm, with ghost-like nuclei (Fig. 2*A*). In contrast, IL-6 treated cells displayed highly fluorescent nuclei (Fig. 2*B*). Similarly, nuclear translocation of STAT3 was observed in cells infected with *H. pylori* strain 7.13 (Fig. 2*C*). To assess the dynamics of the process, fluorescence recovery after photobleaching was used. Cells transfected with GFP-tagged STAT3 proteins were targeted with high-intensity laser light, which bleaches GFP but does not affect the function of endogenous STAT3 protein. The movement of nonbleached molecules into the bleached region was then monitored over time to measure the percentage recovery postbleaching. After bacterial infection, the nuclei of STAT3-GFP transfected cells were bleached using 100% laser photon output at 488 nm, and the recovery kinetics was observed. Uninfected cells recover fluorescence of the entire nuclei by 79 $\pm$ 3.3%; however, IL-6 activated cells showed minimal recovery (29 $\pm$ 2.5%; Fig. 2*D*). Similarly, a reduction in recovery of fluorescence was detected in the nuclei of *H. pylori*–infected cells post bleaching (39 $\pm$ 2.6%), indicating that the majority of STAT3-GFP was localized in the nucleus of infected cells, thereby permitting minimal recovery from the cytoplasm postnuclear bleaching. Taken together, these results indicate that *H. pylori* infection triggers STAT3 nuclear translocation.

***H. pylori* induces STAT3 transcriptional activity.** To test the ability of *H. pylori* to activate STAT3 signaling at the level of transcription, a STAT3-luciferase reporter system was used. As shown in Fig. 2*D*, IL-6 treatment of p950M4-transfected cells enhanced luciferase activity relative to control cells. Similarly, p950M4-transfected cells infected with *H. pylori* strain 60190 showed an increase in relative luciferase activity in comparison with transfected, uninfected control cells (Fig. 2*D*). *H. pylori* infection induces comparable levels of transcriptional activity of STAT3 as IL-6 treatment (P = NS), despite promoting a lower level of pSTAT3 (Fig. 3*A*). Therefore, we compared phosphorylation of STAT3 (Ser^{727}), which is thought to regulate maximal transcriptional activity of STAT3-regulated genes, in IL-6–treated and *H. pylori*–infected cells. No differences in levels of STAT3 (Ser^{727}) phosphorylation were seen in whole-cell extracts from IL-6–treated or *H. pylori*–infected cells (Supplementary Fig. S4*B*). However, nuclear extracts collected from IL-6–treated cells showed greater serine pSTAT3 compared with *H. pylori*–infected cells (Supplementary Fig. S4*B*).

***H. pylori*–mediated STAT3 activation is CagA-dependent.** Because infection with CagA is associated with an increased risk for the development of gastric cancer, we next assessed the role of this effector protein in *H. pylori*–mediated STAT3 activation. Infection with *cagA* isogenic mutants of strain 61090 failed to activate STAT3 (Fig. 3*A*). Similarly, *cagE* mutants, possessing a disrupted type IV secretion system, were also unable to induce STAT3 phosphorylation during infection. In addition, infection with heat-killed bacteria, which destroys heat-labile proteins, such as CagA, but does not affect lipopolysaccharide, resulted in an inhibition of *H. pylori*–mediated STAT3 activation (Supplementary Fig. S5). These findings were confirmed using an additional *H. pylori* Cag+ isolate, strain 251, and its type IV secretion system mutant lacking *cagM* (Supplementary Fig. S6).

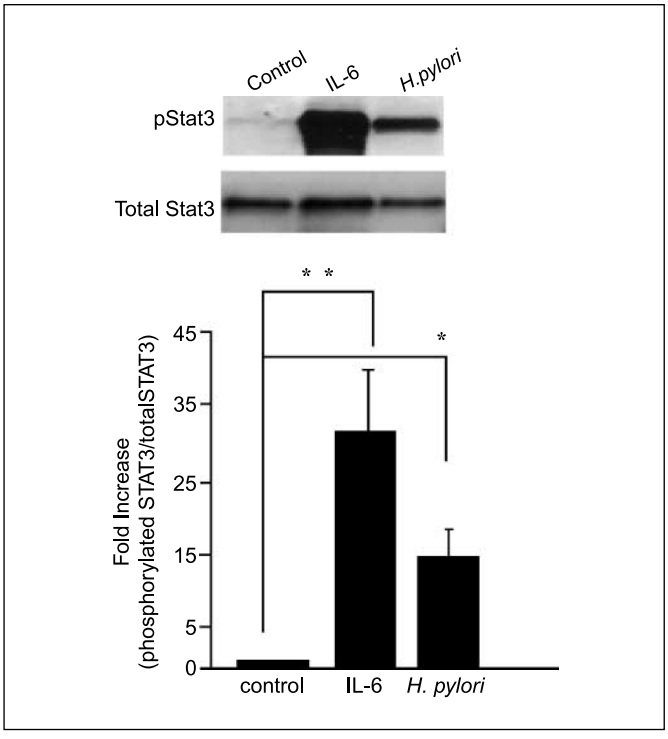

Figure 1. *H. pylori* promotes phosphorylation of STAT3 pathway. Lysates obtained from untreated HEp-2 cells, cells incubated with IL-6 (100 ng/mL, 30 min), or cells infected with *H. pylori* 60190 (wt; MOI, 100:1) for 4 h were used for immunoblotting to detect changes in phosphorylated and native STAT3. The graph represents densitometric analysis of the bands obtained for each protein signal normalized to native STAT3. Fold increase given as a ratio of control pSTAT3/STAT3. *Columns,* mean; *bars,* SE. **, $P < 0.01$; *, $P < 0.05$, using the Student's t test (n = 8).

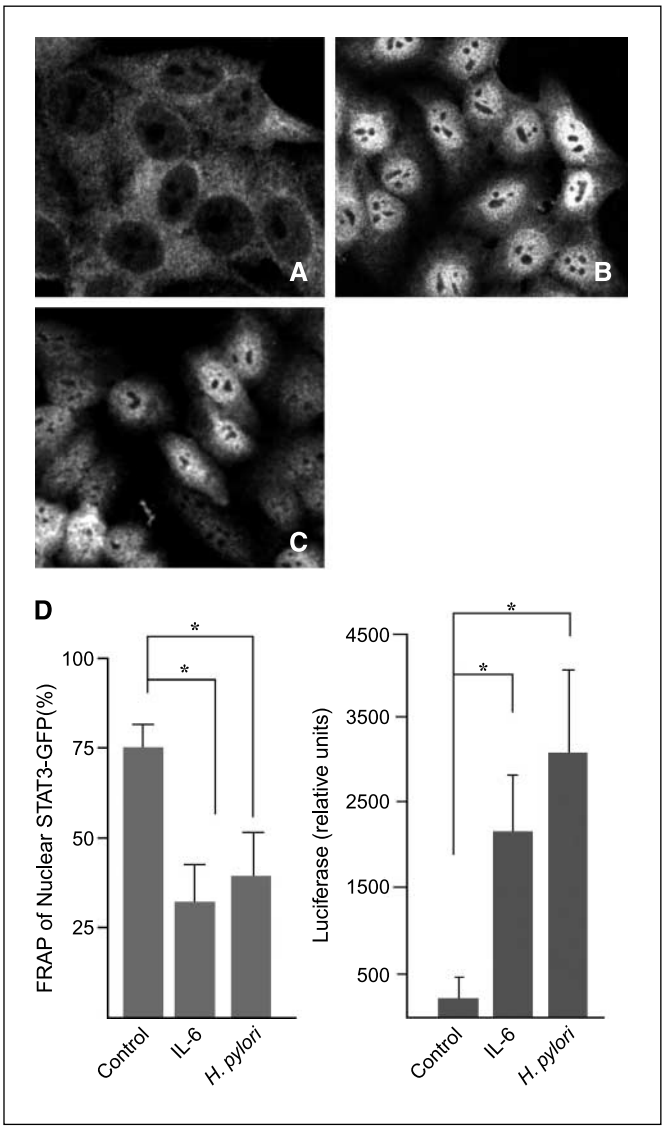

Figure 2. *H. pylori* induces STAT3 nuclear translocation and transcriptional activation in a CagA-dependent manner. *A-C,* HEp-2 cells were treated with culture media (*A*), IL-6 for 30 min (*B*), or infected with *H. pylori* strain 7.13 (*C*) for 4 h. Fixed cells were stained with anti-STAT3 and donkey anti-mouse Cy3 conjugated secondary antibodies. Confocal images were taken of representative cells for each treatment. *D,* whole nuclei of uninfected, IL-6–treated, and *H. pylori*–infected STAT3-GFP transfected cells were bleached, and the percentage recovery of fluorescence was measured relative to the initial values. Six cells for each group were analyzed. *, $P < 0.05$, using the Student's *t* test ($n = 4$). HEp-2 cells were transfected with luciferase reporter constructs containing three repeat STAT3 DNA binding domains, p950m4, or control pSTAT3 plasmids. Transfected cells were treated with IL-6 or infected with *H. pylori* strain 60190 for 48 h, and luciferase activity was measured and normalized against *Renilla* luciferase activity. *, $P < 0.05$, using the Student's *t* test ($n = 3$).

In addition, cells infected with the 7.13 *cagA* mutant (Fig. 3*B, iii*) did not display nuclear STAT3 immunolabeling. Furthermore, HEp-2 cells transfected with CagA-GFP for 20 hours displayed STAT3 activation as assessed by Western blotting for pSTAT3 (Fig. 3*C*) compared with cells transfected with GFP alone. Taken together, these findings indicate that CagA translocation is essential for STAT3 activation.

CagA− mediated STAT3 activation is independent of tyrosine phosphorylation. To determine if tyrosine phosphorylation of the CagA EPIYA motif is required to induce STAT3 phosphorylation, we used an *H. pylori cagA* EPISA mutant, which cannot undergo tyrosine phosphorylation due to a tyrosine (Y) to serine (S) substitution. Infection of HEp-2 cells with either the wt parental strain G27 or the EPISA mutant induced comparable levels of STAT3 phosphorylation (Fig. 4*A*). To confirm that the *cagA* EPISA mutant did not undergo tyrosine phosphorylation, the same whole-cell lysates already probed for pSTAT3 (shown in Fig. 4*A*) were immunoblotted for the presence of a tyrosine phosphorylated protein at molecular weight of CagA (128–144 kDa; ref. 3). As depicted in Fig. 4*B*, the *cagA* EPISA mutant injects CagA with a shift in the molecular weight, as has been shown previously (17). However, unlike injected CagA from the wt G27 strain, tyrosine phosphorylation of the CagA EPISA mutant protein was not detected (Fig. 4*B*).

IL-6R and gp130 are pivotal for *H. pylori* STAT3 activation. To determine the requirement for IL-6Rs in *H. pylori*–mediated STAT3 activation, Sant7, a highly specific receptor antagonist, was used (15). In cells preincubated with Sant7, IL-6–mediated pSTAT3 was significantly reduced (Fig. 5*A*). Similarly, Sant7 completely abrogated the pSTAT3 signal mediated by *H. pylori* infection. Next, an anti-gp130 monoclonal antibody (mAb; ref. 15), which prevents receptor dimerization and activation of the receptor, was used. As shown previously (15), IL-6–induced STAT3 activation was inhibited by the anti-gp130 mAb. Similarly, *H. pylori*–induced STAT3 phosphorylation was eliminated by the anti-gp130 mAb (Fig. 5*B*). Taken together, these findings indicate that both the IL-6R and the gp130 receptor subunits were required for *H. pylori*–mediated STAT3 phosphorylation.

Interaction between CagA and gp130 receptor. To determine if there was a direct interaction between CagA and the gp130 receptor, we attempted to perform coimmunoprecipitation experiments in cells transfected with CagA-GFP and gp130-CFP. Although we were able to coimmunoprecipitate CagA and SHP-2 (Supplementary Fig. S7), a known interacting partner of CagA, we were unable to coimmunoprecipitate gp130 with CagA, indicating that CagA likely does not interact directly with gp130 (data not shown).

***H. pylori*–mediated STAT3 activation is IL-6, IL-11, and LIF independent.** Because both IL-6 and IL-11 can induce STAT3 activation through the gp-130 receptor, we next determined if autocrine activation by IL-6 or IL-11 was involved. IL-6 was measured in culture media from cells infected with either *H. pylori* strain 251 or the *cagM* mutant. IL-6 was undetectable in three separate groups of control HEp-2 cells and *cagM*-infected cells. In *H. pylori* wt infected cells, minimal IL-6 was detected (19.22 pg/mL; Supplementary Table S2). Furthermore, this concentration of IL-6 was insufficient to activate STAT3 signaling (Supplementary Fig. S8). To confirm that *H. pylori*–induced STAT3 activation was independent of IL-6, we used a neutralizing anti–IL-6 antibody. Upon preincubation with the anti–IL-6 antibody, the degree of IL-6–mediated pSTAT3 was significantly reduced (Fig. 5*C*). In contrast, *H. pylori* strains 60190 and 251 still induced STAT3 phosphorylation in the presence of the neutralizing antibody. These findings indicate that autocrine activation of STAT3 by IL-6 was not involved in *H. pylori*–mediated STAT3 phosphorylation. In addition, wt *H. pylori* infection of HEp-2 cells did not result in an increase in IL-11 in culture supernatants (Supplementary Table S2). Furthermore, the sant7 inhibitor that blocks IL-6 and *H. pylori*–mediated STAT3 activation had no effect on IL-11–mediated STAT3 activation (Supplementary Fig. S9).

Furthermore, LIF, a known activator of the STAT3 signaling pathway, was not increased in supernatants collected from *H. pylori*–infected cells (Supplementary Table S2). These results suggest that *H. pylori*–mediated STAT3 activation occurs independently of IL-6, IL-11, and LIF.

A gerbil-adapted carcinogenic CagA+ strain activates STAT3 signaling *in vivo*. Infection with *H. pylori* strain 7.13 induces dysplasia and gastric adenocarcinoma in Mongolian gerbils (14). To determine if *H. pylori* induced STAT3 activation *in vivo*, gerbils were infected with wt strain 7.13 or sham infected (Fig. 6) and sacrificed at 6 or 12 weeks. Gastric tissue lysates obtained from sham-infected animals displayed minimal pSTAT3. In marked contrast, gastric tissue lysates obtained from gerbils infected with wt strain 7.13 displayed increased pSTAT3 after both 6 weeks (Supplementary Fig. S10) and 12 weeks of infection (Fig. 6). To determine if CagA was required for STAT3 activation *in vivo*, we compared STAT3 activation in gastric tissue lysates obtained from gerbils infected with the noncarcinogenic isogenic 7.13 *cagA* mutant (18). As shown previously, CagA+ infected gerbils showed a higher degree of chronic antral inflammation compared with CagA− infected animals; however, there was greater colonization detected in CagA− infected gerbil stomachs (Fig. 6*B, i–ii* and Supplementary Fig. S11). In contrast to wt-infected gerbils, after 12 weeks of infection, pSTAT3 activation was not detected in gerbils infected with the *cagA* mutant strain (Fig. 6*A*). These findings indicate that infection with the known carcinogenic *H. pylori* strain 7.13 (14) induces STAT3 activation in a CagA-dependent manner. To determine the specific cell types exhibiting STAT3 activation, immunohistochemistry was performed on gastric tissue sections. STAT3 nuclear translocation was detected in gastric epithelial cells in a patchy distribution in the antrum of stomachs from CagA+ *H. pylori*–infected animals (Fig. 6*C, iv*). In addition, nuclear STAT3 was detected in inflammatory cells within infiltrates (data not shown). In marked contrast, nuclear STAT3 staining was not detected in gastric tissue obtained from sham-infected or *H. pylori* CagA− infected gerbils (Fig. 6*C, ii, vi*).

Discussion

Although current evidence strongly supports a role for STAT3 activation in the development of gastric cancer, the exact mechanism of STAT3 activation is still unknown. Here, we show that infection with *H. pylori*, the single, most important risk factor for the development of gastric cancer, induces STAT3 activation both *in vitro* and *in vivo*. In addition, our studies define a role for the cancer-associated effector CagA, independent of tyrosine phosphorylation, in STAT3 activation.

We have shown that *H. pylori*–mediated STAT3 activation occurs at the IL-6R level but is independent of the known activation ligands IL-6, IL-11, and LIF, indicating a novel mechanism involving the interaction of both host receptors and CagA. Previous studies indicate that forced dimerization of the gp130 receptor promotes STAT3 activation independent of the IL-6 cytokine (19). Therefore, we hypothesize that CagA modulates STAT3 activation by promoting receptor dimerization, either directly or indirectly. In support of this contention, recent evidence indicates that CagA may interact with several membrane-associated proteins and signaling molecules. For example, Churin and colleagues (5) showed that CagA in a tyrosine phosphorylation-independent manner interacted directly with c-Met in AGS gastric epithelial cells. Mimuro and colleagues (4) showed that CagA, independent of its EPIYA tyrosine phosphorylation motif, associated with the intracellular signaling molecule Grb2. In addition, Amieva and colleagues (6) showed that in addition to altering the location ZO-1 and JAM, CagA, independent of phosphorylation, also altered localization of apical and basolateral membrane proteins in Madin-Darby canine kidney cells (20). Based on our findings, we hypothesize a similar mechanism whereby CagA triggers clustering of the IL-6 and gp130 membrane receptors, favoring STAT3 activation observed

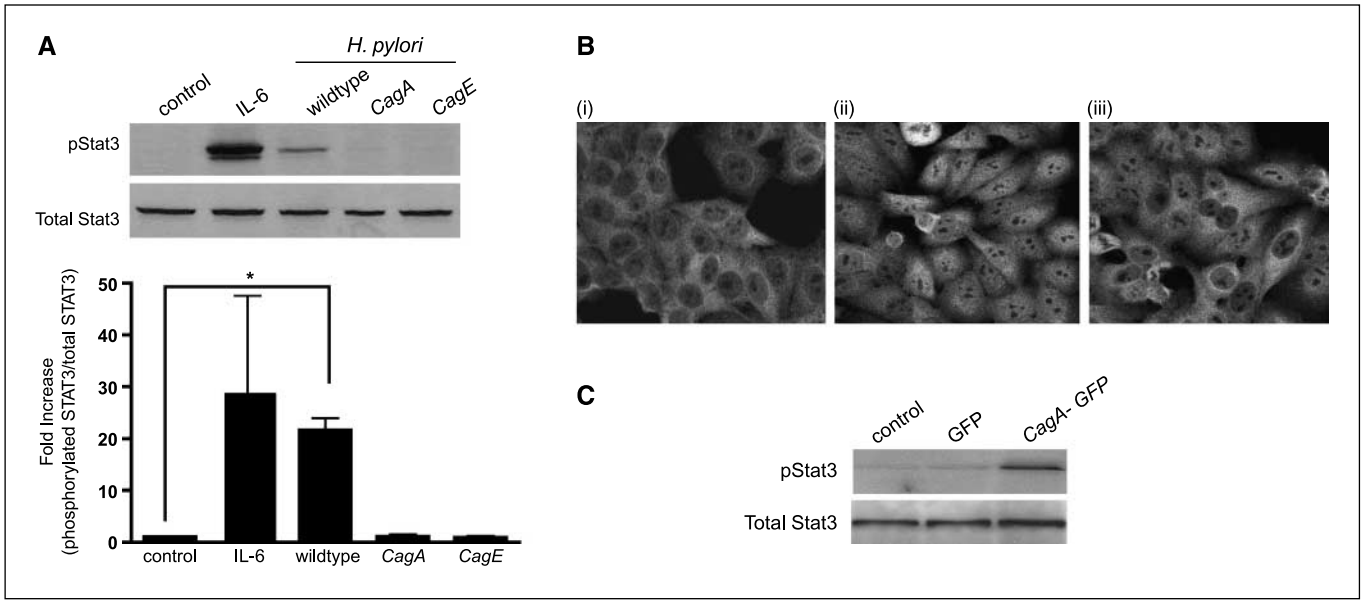

Figure 3. *H. pylori*–mediated STAT3 activation is CagA-dependent. *A,* HEp-2 cells were infected with either *H. pylori* strain 60190, its isogenic *cagA* mutant, or the type IV secretion system mutant *cagE* (MOI, 100:1; for 4 h). Whole-cell lysates were collected and probed for STAT3 activation. Untreated and IL-6–treated cells (50 ng/mL) served as controls. Graph depicts the densitometric analysis for pSTAT3 bands relative to the native STAT3 protein. *, $P < 0.05$, using the Student's *t* test ($n = 4$). *B,* untreated control (*i*), *H. pylori* wt (*ii*), or *cagA* mutant (*iii*) infected HEp-2 cells were immunolabeled for STAT3, and images were obtained using confocal microscopy. *C,* HEp-2 cells were transfected with untagged GFP or CagA-GFP for 20 h, and cell lysates were collected and probed for pSTAT3.

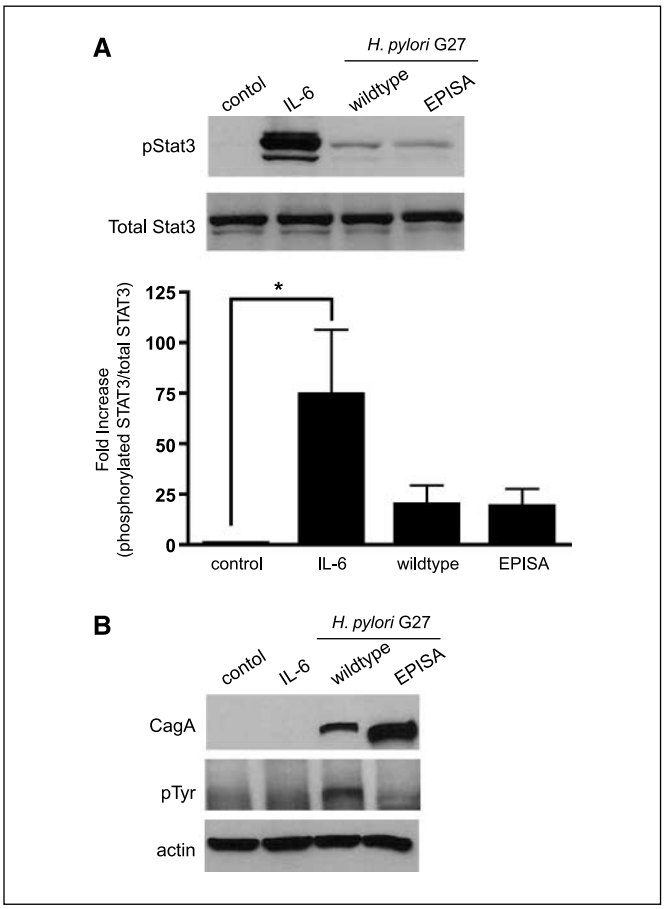

Figure 4. CagA-dependent STAT3 activation does not require tyrosine phosphorylation of CagA. *A,* cells were infected with strain G27 or its *cagA* EPISA mutant. Cell lysates were probed for pSTAT3. Graph depicts the density of pSTAT3 protein bands normalized to native STAT3 detected in each treatment. *, $P < 0.05$ using the Student's *t* test ($n = 6$). *B,* lysates initially probed for pSTAT3 were subsequently analyzed by immunoblotting using a tyrosine phosphorylation-specific antibody to detect the presence of tyrosine phosphorylated CagA.

during *H. pylori* infection. Based on the results of our coimmunoprecipitation studies, there does not seem to be a direct interaction between CagA and gp-130 to promote gp-130 clustering. Further studies are now required to elucidate the exact mechanism involved.

Other bacterial pathogens can modulate the STAT3 intracellular signaling pathway, likely to promote infection. In contrast to our findings, the majority of these bacterial pathogens modulate STAT3 activation via autocrine activation by IL-6. For example, *Listeria monocytogenes* induces STAT3 activation in an IL-6–dependent manner, in Kupffer cells, during the early stages of infection (21). Similarly, *Escherichia coli*–induced pneumonia is accompanied by an increase in IL-6, leading to the activation of STAT3 in the lungs of infected mice, which facilitates improved bacterial clearance (22). Lin and colleagues showed that *Salmonella enterica* serovar *Typhimurium* activates STAT3 in leukocytes and macrophages early during infection and hypothesized that STAT3 activation would reduce the initial destructive inflammatory response (23). However, the mechanism responsible for *Salmonella*-mediated STAT3 activation in these immune cells was independent of IL-6 but was not defined.

To promote their survival, many pathogens use techniques to commandeer host cell signal transduction responses. This is particularly important for organisms that promote chronic infection, such as *H. pylori*. We have previously shown that *H. pylori* alters other STAT signaling pathways, thereby modulating host immune responses. For example, *H. pylori* infection does not, by itself, affect STAT1 activation but disrupts IFN-induced STAT1 activation in

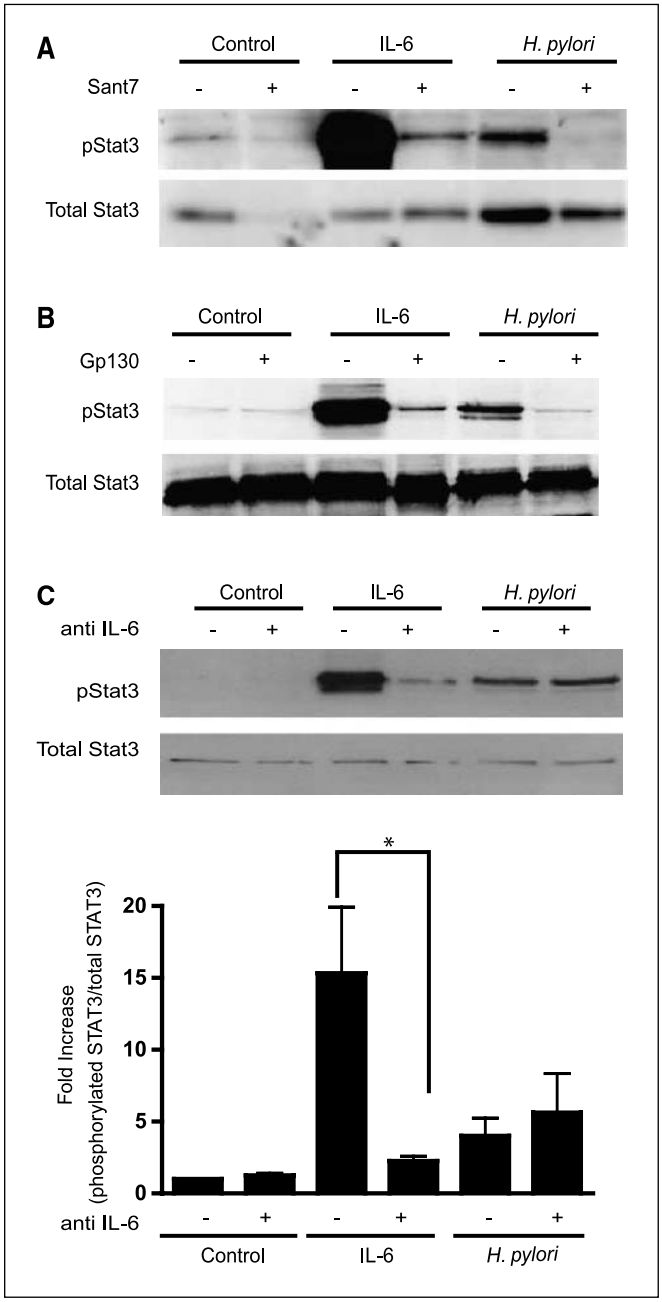

Figure 5. *H. pylori*–mediated STAT3 activation requires the IL-6R and gp130 receptor but is independent of the IL-6 cytokine. *A,* cells were preincubated with IL-6R superantagonist sant7 before incubation with IL-6 (50 ng/mL, 30 min) or infection with strain 60190. Lysates were probed for pSTAT3 and native STAT3 protein. Representative of three independent experiments. *B,* an anti-gp130 blocking antibody was incubated with cells before either *H. pylori* infection or incubation with IL-6, and cell lysates were obtained and immunoblotted for pSTAT3. Representative of three independent experiments. *C,* HEp-2 cells were treated with neutralizing IL-6 antibody followed by infection with strain 60190. Whole-cell lysates were collected and probed for pSTAT3 via Western blotting. Densitometric analysis showing the ratio of pSTAT3 normalized to native STAT3 was performed and represented in the graph. *, $P < 0.05$, using Student's *t* test ($n = 4$).

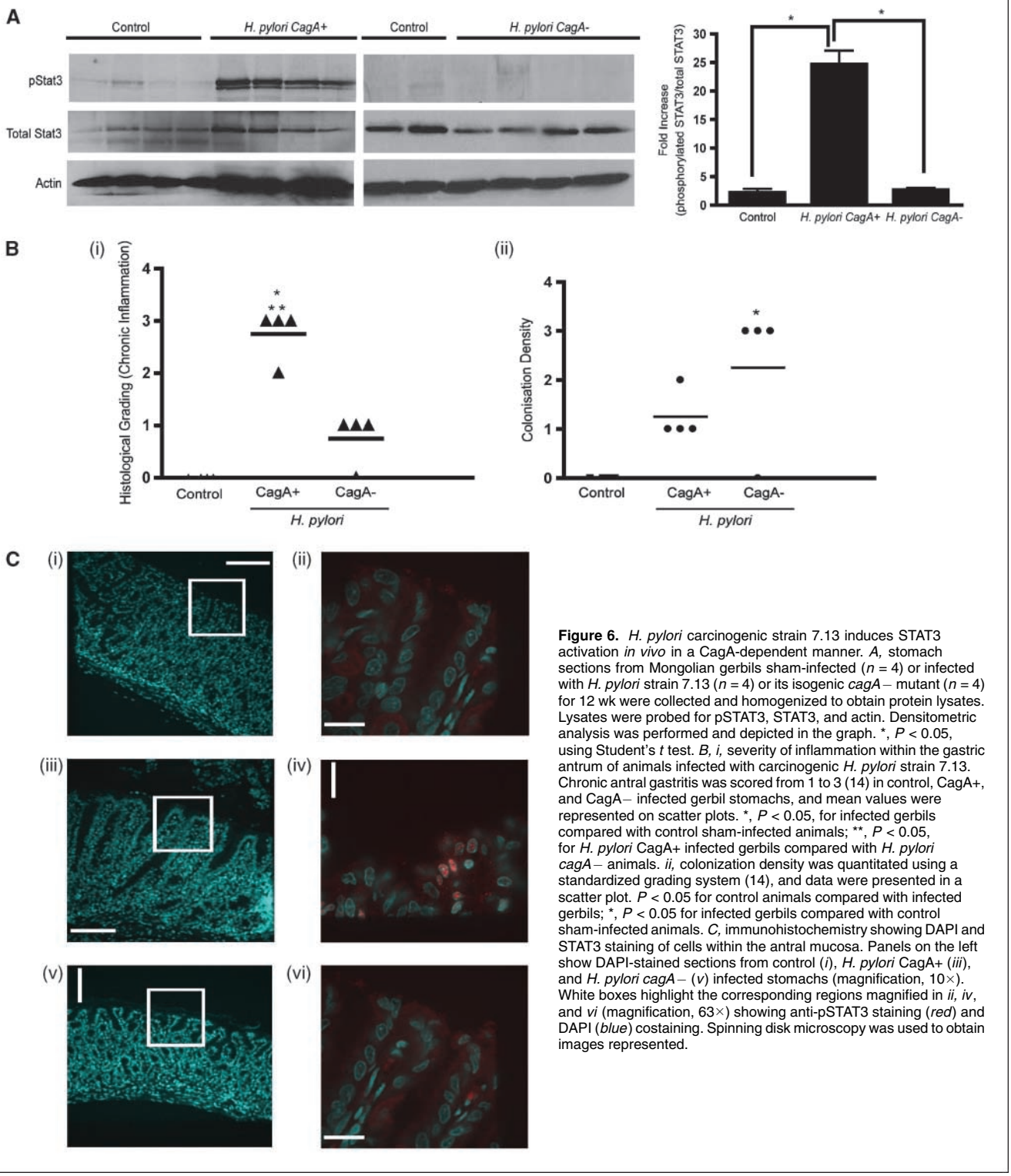

Figure 6. *H. pylori* carcinogenic strain 7.13 induces STAT3 activation *in vivo* in a CagA-dependent manner. *A,* stomach sections from Mongolian gerbils sham-infected ($n = 4$) or infected with *H. pylori* strain 7.13 ($n = 4$) or its isogenic *cagA*− mutant ($n = 4$) for 12 wk were collected and homogenized to obtain protein lysates. Lysates were probed for pSTAT3, STAT3, and actin. Densitometric analysis was performed and depicted in the graph. *, $P < 0.05$, using Student's *t* test. *B, i,* severity of inflammation within the gastric antrum of animals infected with carcinogenic *H. pylori* strain 7.13. Chronic antral gastritis was scored from 1 to 3 (14) in control, CagA+, and CagA− infected gerbil stomachs, and mean values were represented on scatter plots. *, $P < 0.05$, for infected gerbils compared with control sham-infected animals; **, $P < 0.05$, for *H. pylori* CagA+ infected gerbils compared with *H. pylori cagA*− animals. *ii,* colonization density was quantitated using a standardized grading system (14), and data were presented in a scatter plot. $P < 0.05$ for control animals compared with infected gerbils; *, $P < 0.05$ for infected gerbils compared with control sham-infected animals. *C,* immunohistochemistry showing DAPI and STAT3 staining of cells within the antral mucosa. Panels on the left show DAPI-stained sections from control (*i*), *H. pylori* CagA+ (*iii*), and *H. pylori cagA*− (*v*) infected stomachs (magnification, 10×). White boxes highlight the corresponding regions magnified in *ii, iv*, and *vi* (magnification, 63×) showing anti-pSTAT3 staining (*red*) and DAPI (*blue*) costaining. Spinning disk microscopy was used to obtain images represented.

epithelial cells, which could lead to a reduction in the Th1 immune response (24). Of interest, reciprocal interactions between STAT1 and STAT3 by several proposed mechanisms have been described (25). Therefore, it remains possible that, as yet unidentified, effects on STAT1 may enhance *H. pylori*–mediated STAT3 transcriptional activity, providing a possible explanation for the comparable activation in *H. pylori*–treated and IL-6–treated cells.

H. pylori also disrupts IL-4–mediated STAT6 signaling in epithelial cells, inhibiting a Th2 immune response, which is important for eliminating the pathogen (26). *H. pylori*–mediated disruption of both STAT1 and STAT6 occurs in a *cagA, cagE*, and *vacA* independent manner. In contrast, in the present study, the injection of CagA is essential to facilitate STAT3 activation. In addition to the direct role of STAT3 in tumorigenesis, STAT3 is well recognized to facilitate

immune evasion of tumors at many levels, including suppressing proinflammatory responses by inhibiting dendritic cell maturation and promoting development of T-regulatory cells (8). Of interest, recent evidence indicates that the insufficient immune response observed during *H. pylori* infection may be mediated, in part, by both abnormal T-regulatory cells (27, 28) and inhibition of dendritic cell activation (29). In contrast to playing a role in immune surveillance, seemingly paradoxically, STAT3 has also been implicated in modulating certain inflammatory responses that promote cancer, including both inhibition of IL-12 and up-regulation of IL-23 (8). In this study, we detected nuclear STAT3 both in epithelial cells and in inflammatory infiltrates of CagA+ infected gerbils. Thus, *H. pylori*–mediated STAT3 activation may facilitate both immune evasion and procarcinogenic inflammatory responses *in vivo*.

Our findings of CagA-mediated activation of STAT3 in gastric epithelial cells in *H. pylori*–infected gerbils, which develop gastric adenocarcinoma in a CagA-dependent manner (18), raises the hypothesis that STAT3 activation plays a role in oncogenesis in this model. In support of our *in vivo* findings, a recent study from Jackson and colleagues indicates that STAT3 activation is also detected in gastric tissues obtained from *H. pylori*–infected human subjects (30). In this study, similar to our results, STAT3 activation was augmented in subjects infected with a CagA-positive strain. A variety of functional effects are attributed to the oncogenic potential of STAT3, including proliferation, apoptosis, angiogenesis, invasion, migration, and disruption of immune surveillance (7). In contrast, inhibiting STAT3 activation in tumor cells promotes cell death, inhibits angiogenesis, and triggers antitumor immune responses (7). Furthermore, tumor cells seem to be more sensitive to these effects compared with normal cells (7, 8). Thus, STAT3 may represent an ideal target for cancer therapy. Our studies indicate that the Mongolian gerbil model may prove useful to more precisely define the role of STAT3 in the multistep process of gastric carcinogenesis and the effect of STAT3 inhibition on lesion progression.

In conclusion, this study identifies the *H. pylori* effector protein CagA as potentially enhancing the risk for gastric cancer by increasing STAT3 signaling in epithelial cells. The prognosis for gastric cancer is poor with a limited 5-year survival rate (1). Currently, there is no conclusive evidence that eradication of *H. pylori* infection prevents the development of gastric cancer (31). Our results indicate that inhibition of STAT3 activation may be a viable therapy for *H. pylori*–mediated carcinogenesis. Thus, the findings from our studies set the stage for ongoing investigations, addressing the efficacy of STAT3 inhibition for chemoprevention during *H. pylori*–mediated gastric carcinogenesis.

Disclosure of Potential Conflicts of Interest

No potential conflicts of interest were disclosed.

Acknowledgments

Received 3/29/2008; revised 10/9/2008; accepted 10/13/2008.

Grant support: Canadian Institute for Health and Research operating grant, Ontario Ministry of Research and Innovation Early Researcher Award (N.L. Jones), and grants NIH DK 58587, NIH CA 77955, and NIH DK 73902 (R.M. Peek, Jr.).

The costs of publication of this article were defrayed in part by the payment of page charges. This article must therefore be hereby marked *advertisement* in accordance with 18 U.S.C. Section 1734 solely to indicate this fact.

References

1. Peek RM, Jr., Crabtree JE. *Helicobacter* infection and gastric neoplasia. J Pathol 2006;208:233–48.
2. Kusters JG, van Vliet AH, Kuipers EJ. Pathogenesis of *Helicobacter pylori* infection. Clin Microbiol Rev 2006;3: 449–90.
3. Hatakeyama M. Oncogenic mechanisms of the *Helicobacter pylori* CagA protein. Nat Rev Cancer 2004;4: 688–94.
4. Mimuro H, Suzuki T, Tanaka J, Asahi M, Haas R, Sasakawa C. Grb2 is a key mediator of *Helicobacter pylori* CagA protein activities. Mol Cell 2000;10:745–55.
5. Churin Y, Al Ghoul L, Kepp O, Meyer TF, Birchmeier W, Naumann MJ. *Helicobacter pylori* CagA protein targets the c-Met receptor and enhances the motogenic response. Cell Biol 2003;161:249–55.
6. Amieva MR, Vogelmann R, Covacci A, Tompkins LS, Nelson WJ, Falkow S. Disruption of the epithelial apical-junctional complex by *Helicobacter pylori* CagA. Science 2003;300:1430–4.
7. Yu H, Jove R. The STATs of cancer-new molecular targets come of age. Nat Rev Cancer 2004;4:97–105.
8. Yu H, Kortylewski M, Pardoll D. Crosstalk between cancer and immune cells: role of STAT3 in the tumour microenvironment. Nat Rev Immunol 2007;7:41–5.
9. Bromberg JF, Wrzeszczynska MH, Devgan G, et al. Stat3 as an oncogene. Cell 1999;98:295–303.
10. Kanda N, Seno H, Konda Y, Marusawa H, et al. STAT3 is constitutively activated and supports cell survival in association with survivin expression in gastric cancer cells. Oncogene 2004;23:4921–9.
11. Judd LM, Alderman BM, Howlett M, et al. Gastric cancer development in mice lacking the SHP2 binding site on the IL-6 family co-receptor gp130. Gastroenterology 2004;126:196–207.
12. Tebbutt NC, Giraud AS, Inglese M, et al. Reciprocal regulation of gastrointestinal homeostasis by SHP2 and STAT-mediated trefoil gene activation in gp130 mutant mice. Nat Med 2002;8:1089–97.
13. Judd LM, Bredin K, Kalantzis A, Jenkins BJ, Ernst M, Giraud AS. STAT3 activation regulates growth, inflammation, and vascularization in a mouse model of gastric tumorigenesis. Gastroenterology 2006;131:1073–85.
14. Franco AT, Israel DA, Washington MK, et al. Activation of β-catenin by carcinogenic *Helicobacter pylori*. Proc Natl Acad Sci U S A 2005;102:10646–51.
15. Chatterjee M, Honemann D, Lentzsch S, et al. In the presence of bone marrow stromal cells human multiple myeloma cells become independent of the IL-6/gp130/STAT3 pathway. Blood 2006;100:3311–8.
16. Shah M, Patel K, Mukhopadhyay S, Xu F, Guo G, Sehgal PB. Membrane-associated STAT3 and PY-STAT3 in the cytoplasm. J Biol Chem 2006;281:7302–8.
17. Stein M, Bagnoli F, Halenbeck R, Rappuoli R, Fantl W, Covacci A. c-Src/Lyn kinases activate *Helicobacter pylori* CagA through tyrosine phosphorylation of the EPIYA motifs. Mol Micro 2002;43:971–80.
18. Franco A, Johnston E, Krishna U, et al. Regulation of gastric carcinogenesis by *Helicobacter pylori* virulence factors. Cancer Res 2008;68:379–87.
19. Stuhlmann-Laeisz C, Lang S, Chalaris A, et al. Forced dimerization of gp130 leads to constitutive STAT3 activation, cytokine-independent growth, and blockade of differentiation of embryonic stem cells. Mol Biol Cell 2006;17:2986–95.
20. Bagnoli F, Buti L, Tompkins L, Covacci A, Amieva MR. *Helicobacter pylori* CagA induces a transition from polarized to invasive phenotypes in MDCK cells. Proc Natl Acad Sci U S A 2005;102:16339–44.
21. Gregory SH, Wing EJ, Danowski KL, van Rooijen N, Dyer KF, Tweardy DJ. IL-6 produced by Kupffer cells induces STAT protein activation in hepatocytes early during the course of systemic listerial infection. J Immunol 1998;160:6056–61.
22. Jones MR, Quinton LJ, Simms BT, Lupa MM, Kogan MS, Mizgerd JP. Roles of interleukin-6 in activation of STAT proteins and recruitment of neutrophils during *Escherichia coli* pneumonia. J Infect Dis 2006;193: 360–9.
23. Lin T, Bost KL. STAT3 activation in macrophages following infection with Salmonella. Biochem Biophys Res Commun 2004;321:828–34.
24. Mitchell DJ, Huynh HQ, Ceponis PJ, Jones NL, Sherman PM. *Helicobacter pylori* disrupts STAT1-mediated γ interferon-induced signal transduction in epithelial cells. Infect Immun 2004;72:537–45.
25. Regis G, Pensa S, Boselli D, Novelli F, Poll V. Ups and downs: the STAT1:STAT3 seesaw of Interferon and gp130 receptor signaling. Sem Cell Biol Devel 2008;epub ahead of print.
26. Ceponis PJ, McKay DM, Menaker RJ, Galindo-Mata E, Jones NL. *Helicobacter pylori* infection interferes with epithelial Stat6-mediated interleukin-4 signal transduction independent of *cagA*, *cagE*, or *VacA*. J Immunol 2003;171:2035–41.
27. Lundgren A, Stromberg E, Sjoling A, et al. Mucosal FOXP3-expressing CD4+ CD25 high regulatory T cells in *Helicobacter pylori*-infected patients. Infect Immun 2005;73:523–31.
28. Rad R, Brenner L, Bauer S, et al. CD25+/Foxp3+ T cells regulate gastric inflammation and *Helicobacter pylori* colonization *in vivo*. Gastroenterology 2006;131:525–37.
29. Kao JY, Rathinavelu S, Eaton KA, et al. *Helicobacter-pylori* secreted factors inhibit dendritic cell IL-12: a mechanism of ineffective host defense. Am J Physiol Gastrointest Liver Physiol 2006;291:G73–81.
30. Jackson CB, Judd LM, Menheniott TR, et al. Augmented gp130-mediated cytokine signaling accompanies human gastric cancer progression. J Pathol 2007; 213:140–51.
31. Wong BC, Lam SK, Wong WM, et al. China Gastric Cancer Study Group. *Helicobacter pylori* eradication to prevent gastric cancer in a high-risk region of China: a randomized controlled trial. JAMA 2004;291:187–94.